Monatsh Chem (2011) 142:875–880
DOI 10.1007/s00706-011-0544-0

ORIGINAL PAPER

$EuGa_2Sb_2$: a new Zintl phase with four-bonded gallium and three-bonded antimony in a complex three-dimensional $[Ga_2Sb_2]$ polyanion

Inga Schellenberg · Matthias Eul · Rainer Pöttgen

Received: 5 May 2011 / Accepted: 30 May 2011 / Published online: 28 June 2011

Abstract The Zintl phase $EuGa_2Sb_2$ was synthesized by induction melting of the elements in a sealed tantalum tube. The structure was refined from X-ray single-crystal diffractometer data: new type, *Pnma*, $a = 1834.7(3)$, $b = 432.25(7)$, $c = 674.8(1)$ pm, $wR2 = 0.0377$, 875 F^2, and 32 variables. The structure consists of a three-dimensional polyanionic $[Ga_2Sb_2]^{2-}$ network with Ga_2^{4+} dumb-bells (252.1(1) pm Ga1–Ga2) and antimonide anions, leading to the electron-precise description $Eu^{2+}[Ga_2Sb_2]^{2-}$. The divalent character of europium was evident from magnetic susceptibility data and ^{151}Eu Mössbauer spectra. The crystal chemical relationship with the structures of $EuGa_2As_2$ and $BaGa_2Sb_2$ is discussed.

Keywords Zintl phase · Europium · Crystal chemistry

Introduction

A large number of intermetallic RT_2Pn_2 compounds (R = rare earth or alkaline earth metal, T = transition metal, Pn = pnicogen) [1] with tetragonal $ThCr_2Si_2$ and hexagonal $CaAl_2Si_2$ type structure has been studied in the last 40 years because of their interesting magnetic and electrical properties. Prominent examples are the mixed-valence compound $EuNi_2P_2$ [2, 3], superconducting $LaRu_2P_2$ [4], and the spin-density system $BaFe_2As_2$ [5], which becomes superconducting upon partial Ba/K substitution [6]. Chemical bonding in metallic RT_2Pn_2 compounds can often not be described with simple electron counting rules.

With the alkaline earth elements and divalent europium and ytterbium, many 1:2:2 phosphides, arsenides, and antimonides have been reported which fulfil the Zintl concept [7–9]. Typical examples are the electron-precise $CaAl_2Si_2$-type antimonides $EuMn_2Sb_2$, $EuZn_2Sb_2$, $YbMn_2Sb_2$, and $YbZn_2Sb_2$ with divalent cations and antimonide anions [10]. If one substitutes the divalent transition metal by a trivalent main group cation, such electron-precise 1:2:2 pnictides can only be realized if the triel elements form single bonds, leading to different crystal structures. Recent examples are the phosphides RIn_2P_2 (R = Ca, Sr, Ba, Eu) [11, 12], RGa_2P_2 (R = Ca, Ba, Eu) [13–15], the antimonide $BaGa_2Sb_2$ [16], the arsenides RGa_2As_2 (R = Ca, Sr, Eu) [13, 15], and $EuIn_2As_2$ [17]. These pnictides crystallize with different crystal structures with two or three-dimensional $[Ga_2Pn_2]^{2-}$ and $[In_2Pn_2]^{2-}$ polyanions which are separated and charge-balanced by the divalent cations. The various Ga–Ga (240–251 pm) and In–In (274–277 pm) distances are compatible with single bonds. The dimensionality and distortion of the polyanions is a consequence of the slightly differing size of Ca^{2+}, Sr^{2+}, Ba^{2+}, and Eu^{2+}.

In the course of our systematic investigations of $CaAl_2Si_2$-type europium compounds [10, 18, 19] and other EuT_2X_2 intermetallics (T = transition metal, X = element of the 3rd, 4th, or 5th main group) [20–22] we have now obtained $EuGa_2Sb_2$, the missing compound in the RGa_2Sb_2 series with divalent cations. The structure, crystal chemistry, and properties of this antimonide are reported herein.

I. Schellenberg · M. Eul · R. Pöttgen (✉)
Institut für Anorganische und Analytische Chemie,
Westfälische Wilhelms-Universität Münster, Corrensstrasse 30,
48149 Münster, Germany
e-mail: pottgen@uni-muenster.de

Results and discussion

Structure refinement

Careful analysis of the diffractometer data set revealed a primitive orthorhombic lattice, and the systematic extinctions were compatible with space group *Pnma*. The starting atomic positions were obtained from direct methods with Shelxs-97 [23] and the structure was refined using Shelxl-97 [24] (full-matrix least-squares on F^2) with anisotropic atomic displacement parameters for all sites. The occupancy parameters were refined in a separate series of least-squares cycles. All sites were fully occupied within two standard deviations and in the final cycles the ideal values were assumed again. The refinement then smoothly converged to the values listed in Table 1. The final difference Fourier syntheses revealed no significant residues. The refined atomic positions, anisotropic displacement parameters, and interatomic distances are given in Tables 2 and 3.

Crystal chemistry

The antimonide $EuGa_2Sb_2$ crystallizes with a new structure type. It is the missing compound in the RGa_2Sb_2 series with divalent cations. A view of the $EuGa_2Sb_2$ structure along the short unit cell axis is presented in Fig. 1. The gallium and antimony atoms build up a three-dimensional $[Ga_2Sb_2]$ network which leaves larger cages for the europium atoms. Within the network we observe Ga1–Ga2 distances of 252.1(1) pm, slightly longer than in the Ga_2 dumb-bell (244 pm) of the structure of elemental gallium [25], indicating single-bond character. Both crystallographically independent gallium atoms have three antimony neighbors, leading to a distorted tetrahedral coordination (Fig. 2). The various Ga–Sb distances range from 268.3(1) to 288.7(1) pm, close to the sum of the covalent radii [26] of 266 pm, again signalling single bond character.

Considering these two-centre-two-electron bonds and the divalent character (vide infra) of the europium atoms, we end up with an electron precise Zintl formulation $Eu^{2+}[Ga_2]^{4+}[2Sb^{3-}]^{6-}$, or, emphasizing the covalent bond ing between the gallium dimer and the antimonide entities, $Eu^{2+}[Ga_2Sb_2]^{2-}$. The antimony atoms as the most electronegative component in our compound all point toward the europium atoms which fill pairwise cages of coordination number 11 (5 Ga + 6 Sb). Within the $[Ga_2Sb_2]$ network the antimony atoms are well separated.

Table 1 Crystallographic data and structure refinement for $EuGa_2Sb_2$, space group *Pnma*, $Z = 4$

Formula	$EuGa_2Sb_2$
Molar mass/g mol^{-1}	534.90
Lattice parameters/pm (Guinier data)	$a = 1834.7(3)$
	$b = 432.25(7)$
	$c = 674.8(1)$
Cell volume/nm^3	$V = 0.5351$
Density calc./g cm^{-3}	6.64
Crystal size/μm	15 × 20 × 20
$h\ k\ l$ range	±25; ±6; ±9
$\theta_{min}/\theta_{max}$/°	2.2/30.0
Linear absorption coeff./mm^{-1}	31.3
Max./min. transmission	0.272/0.240
No. of reflections	5829
R_{int}	0.1172
No. of independent reflections	875
Reflections used [$I \geq 2\sigma(I)$]	704
$F(000)$, e	908
R factors $R1/wR2$	0.0263/0.0349
$R1/wR2$ all data	0.0413/0.0377
No. of refined parameters	32
Goodness-of-fit	1.04
Extinction coefficient	0.00138(7)
Diff. Fourier residues/e Å^{-3}	−2.27, +1.67

Table 2 Atom positions and anisotropic displacement parameters (pm^2) for $EuGa_2Sb_2$

Atom	x	z	U_{11}	U_{22}	U_{33}	U_{13}	U_{eq}
Eu	0.38486(2)	0.28122(5)	128(2)	118(2)	141(2)	4(1)	129(1)
Ga1	0.20790(5)	0.4632(1)	119(4)	124(4)	141(4)	16(3)	128(2)
Ga2	0.57075(5)	0.0593(1)	146(4)	121(4)	163(4)	24(3)	143(2)
Sb1	0.21296(3)	0.06421(7)	129(2)	102(2)	107(2)	–9(2)	112(1)
Sb2	0.46941(3)	0.73199(7)	138(2)	110(2)	135(2)	–23(2)	128(1)

All atoms lie on Wyckoff positions 4c (x 1/4 z). Coefficients U_{ij} of the anisotropic displacement factor tensor of the atoms are defined by: $-2\pi^2[(ha^*)^2U_{11} + \cdots + 2hka^*b^*U_{12}]$. $U_{12} = U_{23} = 0$

Table 3 Interatomic distances (pm) for $EuGa_2Sb_2$

Eu:	2	Ga2	325.8(1)	Ga2:	1	Ga1	252.1(1)
	2	Sb1	339.7(1)		2	Sb2	268.3(1)
	1	Sb2	341.5(1)		1	Sb2	288.7(1)
	2	Sb2	343.9(1)		2	Eu	325.8(1)
	1	Ga1	347.1(1)		2	Ga2	347.2(1)
	1	Sb1	347.7(1)	Sb1:	2	Ga1	269.1(1)
	2	Ga1	348.9(1)		1	Ga1	269.4(1)
Ga1:	1	Ga2	252.1(1)		2	Eu	339.7(1)
	2	Sb1	269.1(1)		1	Eu	347.7(1)
	1	Sb1	269.4(1)	Sb2:	2	Ga2	268.3(1)
	1	Eu	347.1(1)		1	Ga2	288.7(1)
	2	Eu	348.9(1)		1	Eu	341.5(1)
					2	Eu	343.9(1)

All distances of the first coordination spheres are listed

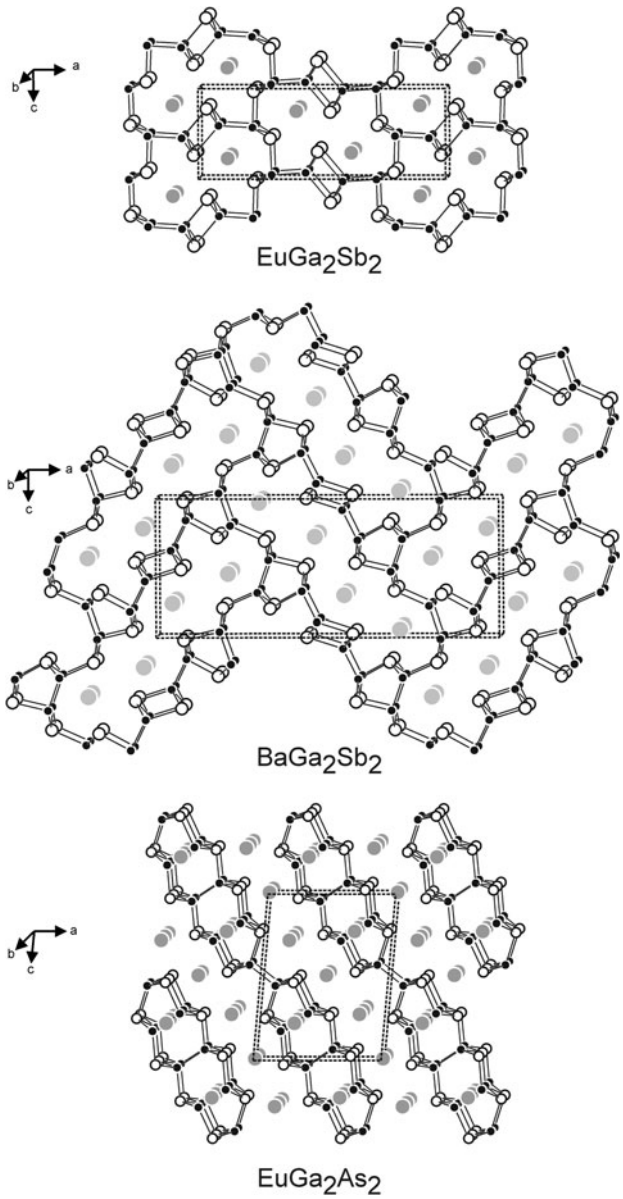

Fig. 1 View of the $EuGa_2Sb_2$, $BaGa_2Sb_2$, and $EuGa_2As_2$ structures along the short unit cell axes. Europium (barium), gallium, and antimony (arsenic) atoms are drawn as medium gray, black filled, and open circles, respectively. The $[Ga_2Sb_2]$ and $[Ga_2As_2]$ polyanions are emphasized

The shortest Sb–Sb distance of 396.7(9) pm cannot be regarded as bonding. Also the europium atoms are well separated. The shortest Eu–Eu distance of 432.25(7) pm corresponds to the *b* lattice parameter.

In Fig. 1 we compare the $[Ga_2Sb_2]$ network of $EuGa_2Sb_2$ with that in $BaGa_2Sb_2$ [16] and with the $[Ga_2As_2]$ network in $EuGa_2As_2$ [13]. The three pnictides are isoelectronic with Ga_2 dumb-bells and Pn^{3-} ions, but their structures are significantly different. With the slightly larger barium atoms one observes larger cavities with four rows of barium cations in one channel compared with two

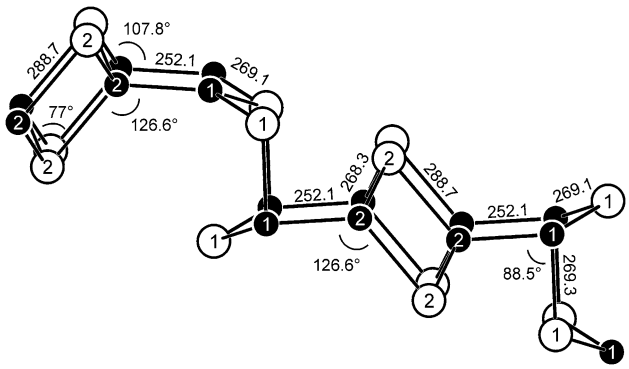

Fig. 2 Cutout of the three-dimensional $[Ga_2Sb_2]^{2-}$ polyanion of $EuGa_2Sb_2$. Gallium and antimony atoms are drawn as black filled circles and open circles, respectively. Relevant interatomic distances (pm) and bond angles (°) are indicated

rows in the europium compound. In going from $EuGa_2Sb_2$ to $EuGa_2As_2$ [13], one reduces the size of the pnictide component, and the resulting $[Ga_2As_2]$ network is now two-dimensional. It is interesting to note that all phosphides and arsenides in these 1:2:2 series have pronounced two-dimensional $[Ga_2Pn_2]$ and $[In_2Pn_2]$ networks, whereas the two antimonides $BaGa_2Sb_2$ [16] and $EuGa_2Sb_2$ have three-dimensional networks.

Magnetic properties

The top panel of Fig. 3 shows the magnetic and inverse magnetic susceptibility (χ and χ^{-1} data) of $EuGa_2Sb_2$ measured at 10 kOe. $EuGa_2Sb_2$ shows Curie–Weiss behaviour above 50 K with an effective magnetic moment $\mu_{eff} = 7.47(1)$ μ_B/Eu atom and a Weiss temperature $\theta_p = 5.5(3)$ K obtained from a fit of $\chi(T) = C/(T - \theta_p)$ in the temperature range of 50–300 K. The effective magnetic moment is somewhat lower than the theoretical value of 7.94 μ_B for a free Eu^{2+} ion, which can be attributed to the presence of GaSb as an identifiable impurity seen in the XRD powder pattern. The positive Weiss temperature is indicative of weak ferromagnetic interactions in the paramagnetic region. The onset of magnetic ordering is visible at around 7 K. To determine the exact ordering temperature, low-field (100 Oe) measurements in the zero-field cooled (ZFC) and field-cooled (FC) mode were performed, as seen in the inset. Here, the antiferromagnetic ordering is clearly evident and the Néel temperature was determined to $T_N = 7.8(5)$ K. There is an upturn in the magnetic susceptibility below 5 K which can most likely be attributed to a spin-reorientation. A minor anomaly is also visible at 6.1(5) K, which coincides with the antiferromagnetic ordering temperature of $Eu_7Ga_8Sb_8$ [27], although this compound could not be detected in the XRD powder pattern.

In the bottom panel of Fig. 3 the magnetization isotherms of $EuGa_2Sb_2$ measured at 5, 15, and 50 K are

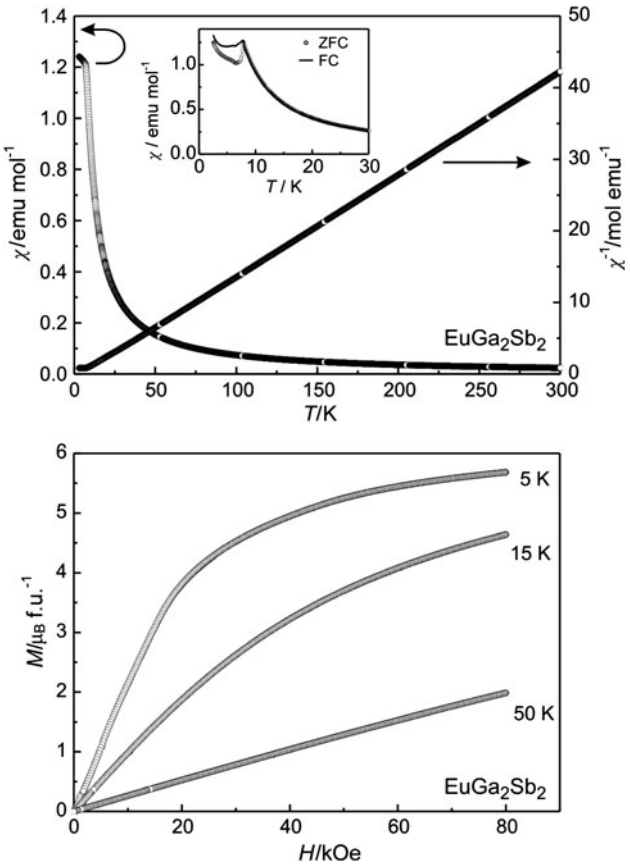

Fig. 3 *Top panel* magnetic and inverse magnetic susceptibility (χ and χ^{-1} data) of $EuGa_2Sb_2$ measured at 10 kOe. *Inset* shows χ data in the low-temperature region measured at 100 Oe in the zero-field-cooled and field-cooled modes. *Bottom panel* magnetization isotherms of $EuGa_2Sb_2$ measured at 5, 15, and 50 K

displayed. At 50 K the magnetization increases linearly with increasing field strength as is expected for a paramagnetic material. At 15 K slight curvature of the magnetization is evident, because of saturation effects at low temperatures and high fields. Below T_N (5 K) the magnetization increases nearly linearly up to approximately 18 kOe and then tends towards saturation. The saturation magnetization of $\mu_{sm} = 5.69(3)$ μ_B/Eu atom at 5 K and 80 kOe is slightly lower than the theoretical value of 7 μ_B for Eu^{2+}. Higher external fields are needed to induce full parallel spin alignment.

Mössbauer spectroscopy

The Mössbauer spectra of the new antimonide $EuGa_2Sb_2$ taken at 77 and 4.2 K are presented in Fig. 4 together with transmission integral fits. The corresponding fitting parameters are listed in Table 4.

The europium spectra are composed of one major resonance at isomer shift values corresponding to divalent europium. The minor component (~5% intensity) in the range of zero velocity is attributed to an Eu^{3+} impurity, formed by surface oxidation. This Eu^{3+} signal is included as a broad Lorentzian line in the fit at both temperatures. The quadrupole interaction decreases from 3.0(2) mm s^{-1} at 77 K to −0.47(5) mm s^{-1} at 4.2 K. At 4.2 K the europium magnetic moments are in an ordered state leading to a magnetic hyperfine field of 21.42(5) T acting on the nuclear spin levels, resulting in clearly visible Zeeman splittings.

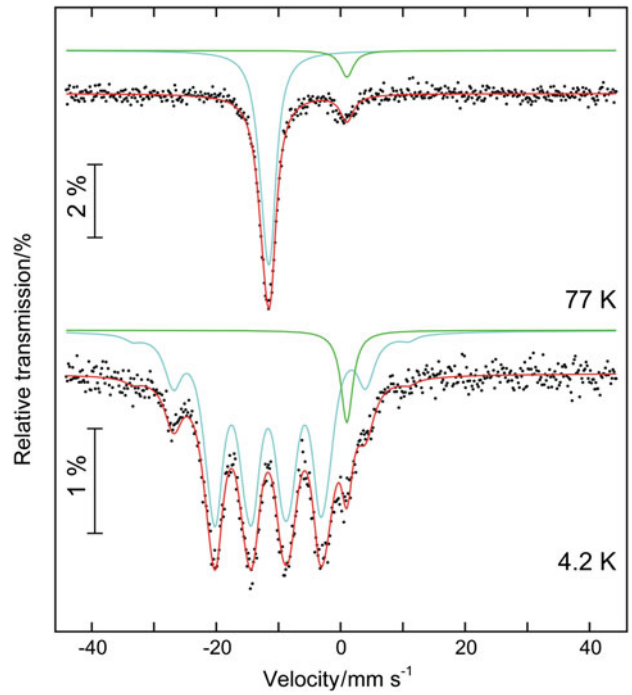

Fig. 4 Experimental and simulated ^{151}Eu Mössbauer spectra of $EuGa_2Sb_2$ at 77 and 4.2 K

Table 4 Fitting parameters of ^{151}Eu Mössbauer spectroscopic measurements of $EuGa_2Sb_2$

T/K	δ/mm s^{-1}	Γ/mm s^{-1}	ΔE_Q/mm s^{-1}	B_h/T
77	–11.72(2)	2.37(7)	3.0(2)	–
4.2	–11.62(2)	2.88(5)	–0.47(5)	21.42(5)

Numbers in parentheses represent the statistical errors in the last digit
δ isomer shift, Γ experimental line width, ΔE_Q electric quadrupole splitting, B_h magnetic hyperfine field

Experimental

Synthesis

Starting materials for the preparation of $EuGa_2Sb_2$ were sublimed ingots of europium (Smart Elements, >99.9%), gallium lumps (Johnson Matthey, >99.9%), and antimony

shots (ABCR, 99.99%). The air and moisture-sensitive europium ingots were kept under argon before the reaction. The argon was purified before use with titanium sponge (870 K), silica gel, and molecular sieves. The elements were weighed in the ideal 1:2:2 atomic ratio and sealed in a tantalum tube under an argon pressure of 800 mbar in an arc melting apparatus [28]. The tantalum tube was subsequently placed in the water-cooled sample chamber of an induction furnace [29] (Hüttinger Elektronik, Freiburg, Germany; type TIG 2.5/300), heated to ca. 1,680 K, and kept at that temperature for 10 min. Finally, the temperature was reduced to 1,180 K, and the sample was annealed at that temperature for another 3 h and then cooled within the furnace after the power was switched off. The temperature was monitored by use of a Sensor Therm Methis MS09 pyrometer with an accuracy of ±30 K. No reaction with the container material was observed. The polycrystalline sample is light grey and stable in air for weeks. Small single crystals have a metallic lustre. By-products (which remained after several variations of the synthetic procedure) were GaSb and a trace of $EuGa_2$.

Scanning electron microscopy

Semiquantitative EDX analyses of the single crystal investigated on the diffractometer and the bulk sample were carried out with a Zeiss EVO MA10 scanning electron microscope with EuF_3, GaP, and Sb as standards. The experimentally observed compositions were close to the ideal composition. No impurity elements were observed.

X-ray diffraction data

The sample was characterized by X-ray powder diffraction using a Guinier camera equipped with an image plate system (Fujifilm, BAS-1800) using Cu $K\alpha_1$ radiation and α-quartz ($a = 491.30$, $c = 540.46$ pm) as an internal standard. The orthorhombic lattice parameters were deduced by least-squares refinement of the powder data. To ensure correct indexing, the experimental pattern was compared with a calculated pattern [30] using the positional parameters obtained from the structure refinement.

Irregularly shaped single crystals were obtained from the annealed sample by mechanical fragmentation. The crystals were glued to quartz fibres by use of beeswax and were characterized by Laue photographs on a Buerger camera (white molybdenum radiation, image plate technique, Fujifilm, BAS-1800) in order to check their suitability for intensity data collection. The data set was collected at room temperature by use of a four-circle diffractometer (CAD4) with graphite-monochromated Mo $K\alpha$ radiation and a scintillation counter with pulse height discrimination. The scans were taken in the $\omega/2\theta$ mode and an empirical absorption correction was applied on the basis of psi-scan data, accompanied by a spherical absorption correction. All relevant crystallographic data and details of the data collection and evaluation are listed in Table 1. Further information on the structure refinement is available from Fachinformationszentrum Karlsruhe, 76344 Eggenstein-Leopoldshafen (Germany), by quoting the registry no. CSD-423030.

Magnetic measurements

For magnetic measurements 9.760 mg of the polycrystalline sample of $EuGa_2Sb_2$ were packed in Kapton foil and attached to a sample holder rod. The measurements were performed using the VSM option of a Quantum Design physical property measurement system (PPMS), in the temperature range 2.5–300 K and with magnetic flux densities up to 80 kOe.

Mössbauer spectroscopy

The 21.53 keV transition of ^{151}Eu with an activity of 130 MBq (2% of the total activity of a $^{151}Sm{:}EuF_3$ source) was used for the Mössbauer spectroscopic experiments, which were conducted in the usual transmission geometry. The measurements were performed with a commercial helium-bath cryostat. The temperature of the absorber was varied between 4.2 K and room temperature, and the source was kept at room temperature. The temperature was monitored by use of a resistance thermometer (±0.5 K accuracy). The sample was enclosed in a small PVC container at a thickness corresponding to approximately 10 mg Mössbauer active element/cm^2.

Acknowledgments This work was financially supported by the Deutsche Forschungsgemeinschaft through SPP 1458 *Hochtemperatursupraleitung in Eisenpnictiden*.

References

1. Villars P, Cenzual K (2010) Pearson's crystal data: crystal structure database for inorganic compounds, release 2009/10. ASM International®, Materials Park
2. Nagarajan R, Sampathkumaran EV, Gupta LC, Vijayaraghavan R, Prabhawalkar V, Bhaktdarshan, Padalia BD (1981) Phys Lett A 84:275
3. Mörsen E, Mosel BD, Müller-Warmuth W, Reehuis M, Jeitschko W (1988) J Phys Chem Solids 49:785
4. Jeitschko W, Glaum R, Boonk L (1987) J Solid State Chem 69:93
5. Rotter M, Tegel M, Johrendt D, Schellenberg I, Hermes W, Pöttgen R (2008) Phys Rev B 78:020503
6. Rotter M, Tegel M, Johrendt D (2008) Phys Rev Lett 101:107006
7. Schäfer H, Eisenmann B, Müller W (1973) Angew Chem Int Ed 12:694
8. Nesper R (1990) Prog Solid State Chem 20:1

9. Kauzlarich SM (1996) Chemistry structure and bonding of Zintl phases and ions. VCH Publishers, New York
10. Schellenberg I, Eul M, Hermes W, Pöttgen R (2010) Z Anorg Allg Chem 636:85
11. Jiang J, Kauzlarich SM (2006) Chem Mater 18:435
12. Rauscher JF, Condron CL, Beault T, Kauzlarich SM, Jensen N, Klavins P, MaQuilon S, Fisk Z, Olmstead MM (2009) Acta Crystallogr C 65:i69
13. Goforth AM, Hope H, Condron CL, Kauzlarich SM, Jensen N, Klavins P, MaQuilon S, Fisk Z (2009) Chem Mater 21:4480
14. He H, Stearrett R, Nowak ER, Bobev S (2010) Inorg Chem 49:7935
15. He H, Stearrett R, Nowak ER, Bobev S (2011) Eur J Inorg Chem. doi:10.1002/ejic.201100065
16. Kim S-J, Kanatzidis MG (2001) Inorg Chem 40:3781
17. Goforth AM, Klavins P, Fettinger JC, Kauzlarich SM (2008) Inorg Chem 47:11048
18. Schellenberg I, Pfannenschmidt U, Eul M, Schwickert C, Pöttgen R (2011) Z Anorg Allg Chem (in press)
19. Nientiedt AT, Lincke H, Rodewald UC, Pöttgen R, Jeitschko W (2011) Z Naturforsch 66b:221
20. Kußmann D, Pöttgen R, Rodewald UC, Rosenhahn C, Mosel BD, Kotzyba G, Künnen B (1999) Z Naturforsch 54b:1155
21. Schellenberg I, Eul M, Pöttgen R (2010) Z Naturforsch 65b:18
22. Schellenberg I, Hermes W, Lidin S, Pöttgen R (2011) Z Kristallogr 226:214
23. Sheldrick GM (1990) SHELXS-97, Program for the Solution of Crystal Structures, University of Göttingen. Acta Crystallogr A46:467
24. Sheldrick GM (2008) SHELXL-97, Program for Crystal Structure Refinement, University of Göttingen. Acta Crystallogr A64:112
25. Donohue J (1974) The structures of the elements. Wiley, New York
26. Emsley J (1999) The elements. Oxford University Press, Oxford
27. Bobev S, Hullmann J, Harmening T, Pöttgen R (2010) Dalton Trans 39:6049
28. Pöttgen R, Gulden T, Simon A (1999) GIT Labor-Fachz 43:133
29. Kußmann D, Hoffmann R-D, Pöttgen R (1998) Z Anorg Allg Chem 624:1727
30. Yvon K, Jeitschko W, Parthé E (1977) J Appl Crystallogr 10:73